Journal of Applied Polymer Science

Removal of Hexavalent Chromium in Wastewater by Polyacrylamide Modified Iron Oxide Nanoparticle

Guihong Lan,[1,2] Xia Hong,[1] Qiang Fan,[1] Bing Luo,[1] Peng Shi,[1] Xiuli Chen[1]

[1]College of Chemistry and Chemical Engineering, Southwest Petroleum University, Chengdu 610500, China

[2]State Key Laboratory of Oil Gas Reservoir Geology and Exploitation, Southwest Petroleum University, Chengdu 610500, China

Correspondence to: G. Lan (E-mail: guihonglan416@sina.com)

ABSTRACT: Iron oxide nanoparticle has been successfully modified by polyacrylamide and the polyacrylamide modified magnetic nanoparticles (PMMNs) were applied to remove Cr(VI) in wastewater. The vibrating sample magnetometer (VSM) spectra indicated the large saturation magnetization and superparamagnetic property of the PMMNs. This made the polyacrylamide modified iron oxide easily separate with liquid phase. Scanning electron microscope (SEM) results showed that both the synthesized iron oxide and the PMMNs were nanoscale. Batch adsorption studies had been carried out to determine the effect of pH, contact time, Cr(VI) initial concentration, and coexisting salts on the adsorption of Cr(VI). Maximum removal (98.30%) was observed from an initial concentration of 100 mg L^{-1} Cr(VI) at pH 3.0, 30°C. This process followed pseudo-second-order kinetics model and the equilibrium time was 40 min. The experimental data fitted the Langmuir isotherm better than Freundlich. Maximum adsorption amount of Cr(VI) by PMMN was 35.186 mg g^{-1}. The effect of coexisting salts on Cr(VI) removal was not apparent even the concentration of salt was 10 times as big as the low concentration, 0.01*M*. It had been proposed that the mechanism of Cr(VI) uptake onto PMMN was adsorption-coupled reduction. © 2014 Wiley Periodicals, Inc. J. Appl. Polym. Sci. **2014**, *131*, 40945.

KEYWORDS: adsorption; kinetics; magnetism and magnetic properties; nanoparticles; nanowires and nanocrystals; polyamides

Received 17 December 2013; accepted 2 May 2014

DOI: 10.1002/app.40945

INTRODUCTION

Cr(VI) exits widely in wastewater of electroplating, leather tanning, pigment, paint, metal, printing, dyeing, and printing industry, etc. It is very dangerous to organism with strong carcinogenic change, teratogenic, mutagenic effects, and strong oxidizing. Besides, it is accredited as one of the 17 kinds of chemicals which are most harmful to human health. So developing an effective, green, fast, and low cost technology for removing Cr(VI) is very urgent.

In recent years, a large number of researchers studied the removal of Cr(VI) from wastewater. Khezami and Capart[1] reported the activated carbon could remove Cr(VI) by adsorption process. Béni et al.[2] found that liquid–liquid extraction could separate Cr(VI) from water with ethyl acetate as extracting agent. Condensed-tannin gel,[3] sodium metabisulfite,[4] and sulfite[5] were reported to be reducing agent for reducing Cr(VI) to Cr(III), then Cr(III) was removed by ion exchange[3] and chemical precipitation,[4,5] respectively. Besides, Barrera et al.[6] reported that electrochemical reduction generated less sludge as chemical process when using Fe^{2+} as reducing agent. These methods generally have the disadvantages of equipment demanding, secondary pollution, and Cr(VI) recovery difficulties. When compared with these methods, adsorption is recognized as an economic, effective, and promising technique to remove Cr(VI).

Organic macromolecular materials are widely used to adsorb metal ions because their numbers of active groups which can adsorb various ions. Most of the Organic macromolecular materials are folcculant. It will accelerate settlement of suspended particles by bridge and adsorption effects. Eisazadeh[7] synthesized polyaniline/poly(vinyl alcohol) for heavy metal uptake and the results was very good. Lignocellulosic substrate[8] extracted from wheat bran and xanthated chitosan[9] were reported to have good properties of removing Cr(VI). Li et al.[10] synthesized polypyrrole/graphene oxide composite nanosheets and found that it exhibited an enhanced properties for Cr(VI) ions removal based on the synergy effect of polypyrrole and graphene oxide. Zhao et al.[11] reported that there were strong complexation reactions between metal ions and $-NH_2$ groups. Furthermore, Li et al.[12] reported the group of $-NH_3^+$ played an important role in the Cr(VI) adsorption. Unnithan et al.[13] synthesized amine-modified polyacrylamide-grafted coconut coir pith. Raji and Anirudhan[14] synthesized polyacrylamide-grafted sawdust. They both reported that after treated with HCl, these materials had a

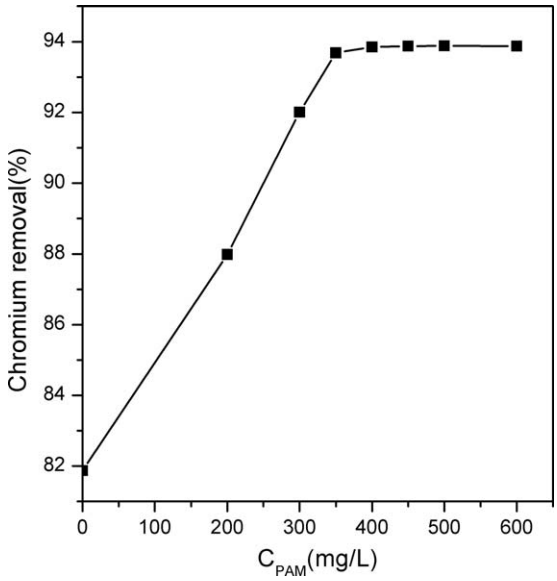

Figure 1. Effect of PAM concentration on the removal of Cr(VI). Cr(VI) concentration, 100 mg L^{-1}; pH 5; contact time, 40 min at 30°C.

$-NH_3^+Cl^-$ group. The $-NH_3^+Cl^-$ group could act as anion exchanger:

$$-NH_3^+Cl^- + HCrO_4^- \rightarrow -NH_3^+ \cdots HCrO_4^- + Cl^- \quad (1)$$

Moreover, Deng and Ting[15] presented that the $-NH_2$ group could be protonated at a certain pH. Then, $-NH_3^+$ could adsorb anionic hexavalent chromium via electrostatic attraction through:

$$-NH_3^+ + HCrO_4^- \rightarrow -NH_3^+ \cdots HCrO_4^- \quad (2)$$

Above them, it is concluded that $-NH_2$ group is of vital importance to Cr(VI) removal.

Magnetic separation has been gradually regarded as a rapid and effective separating technique. It has the advantage that the harmful ingredients can be eliminated from the polluted system together with the magnetic particles by external magnetic field. Furthermore, some magnetic oxide had the ability to adsorb Cr(VI). As Chowdhury et al.[16] reported, there were Fe^{2+} and $FeOH^+$ on the iron oxide surfaces. They would attract negative Cr(VI) species when the solution pH is acidic:

$$-FeOH^+ + HCrO_4^- \rightarrow -FeOH^+ \cdots HCrO_4^- \quad (3)$$

So it will be a quick and efficient adsorption and rapid solid–liquid separation process if we combine the characteristic of organic macromolecular materials and magnetic compound. But unfortunately, relevant report is really rare by far. Anirudhan et al.[17] synthesized iron(III) complex of an amino-functionalized polyacrylamide-grafted lignocellulosics and Zhao et al.[18] found ethylenediamine-functionalized Fe_3O_4 magnetic polymers for removing Cr(VI). They both showed very high adsorption efficiency and easily separating property.

In this study, we report a method of synthetic polyacrylamide modified magnetic nanoparticles (PMMNs) and apply it to remove hexavalent chromium. The effectiveness of PMMN for the removal of hexavalent chromium was demonstrated from lab batch tests and the optimum adsorption conditions were obtained.

Table I. Comparison of Cr(VI) Removal Percentage and Settling Time

Material	Cr(VI) removal percentage (%)	Settling time (s)
Synthesized iron oxide	81.867	240
PMMN (C_{PAM}, 400 mg L^{-1})	97.120	16

EXPERIMENTAL

Materials and Reagents

In this article, all the chemicals were purchased from Kelong chemical reagent factory (Chengdu, China). Among them, $K_2Cr_2O_7$, $FeCl_3{\cdot}6H_2O$, $FeSO_4{\cdot}7H_2O$, NaOH, H_2SO_4, NaCl, $CuSO_4{\cdot}6H_2O$, $ZnSO_4{\cdot}7H_2O$, ammonia, ethanol, acetone, and diphenylcarbazide were of analytical grade. Polyacrylamide (anion, Mr 6×10^6) was chemical pure.

Iron Oxide Nanoparticles Preparation

The iron oxide nanoparticle was prepared in aqueous solution using chemical co-precipitation method[19] with $FeCl_3{\cdot}6H_2O$ and $FeSO_4{\cdot}7H_2O$ as materials, ammonia as precipitant. At room temperature, 5.4 g $FeCl_3{\cdot}6H_2O$ and 2.8 g $FeSO_4{\cdot}7H_2O$ were dissolved in distilled water. Then, 3% ammonia was added in the solution to adjust pH to 10. The solution was continuously stirred (250 rpm) about 30 min. Then, Fe_3O_4 was obtained according to the following equation:

$$Fe^{2+} + 2Fe^{3+} + 8NH_3 \cdot H_2O \rightarrow Fe_3O_4 + 8NH_4^+ + 4H_2O \quad (4)$$

Throughout this process, N_2 was constantly sparged into the solution to prevent oxidation of Fe^{2+}. The black product was separated by external magnetic field (a magnet about 10 cm in diameter) and washed with distilled water and anhydrous ethanol for several times. The final product was dried at 30°C for 1 day.

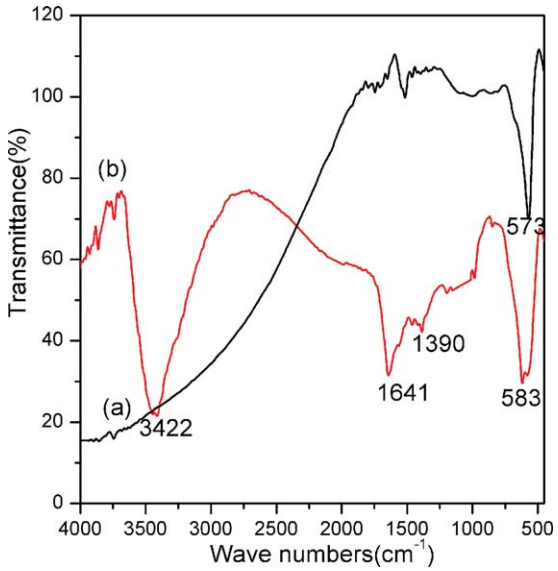

Figure 2. FTIR spectrum of iron oxide (a) and PMMN (b). [Color figure can be viewed in the online issue, which is available at wileyonlinelibrary.com.]

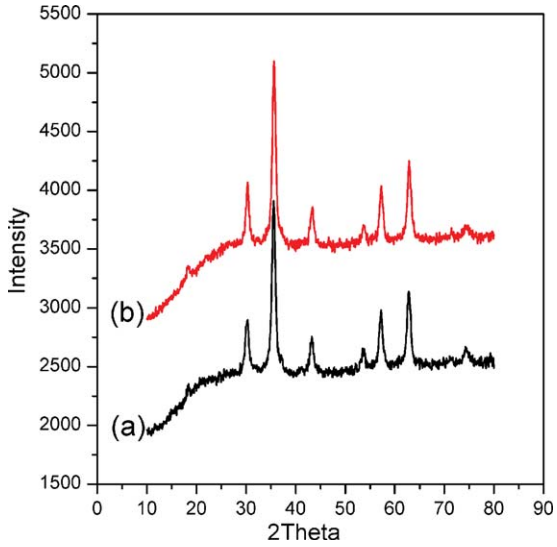

Figure 3. XRD patterns of synthesized iron oxide (a) and PMMN (b). [Color figure can be viewed in the online issue, which is available at wileyonlinelibrary.com.]

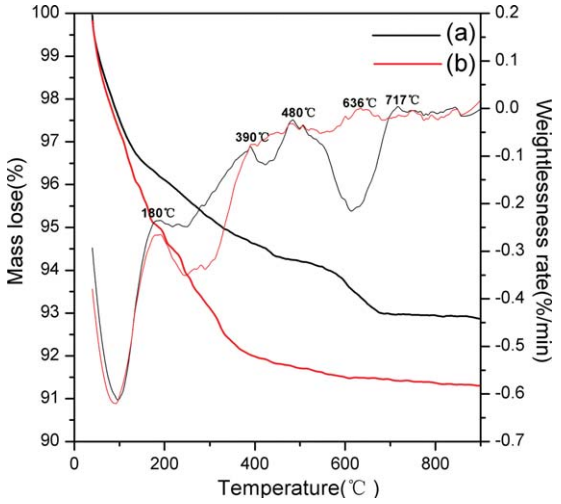

Figure 5. TG/DTG curves of synthesized iron oxide (a) and PMMN (b). [Color figure can be viewed in the online issue, which is available at wileyonlinelibrary.com.]

Synthesis of PMMN

The synthesis of PMMN was carried out with a stirring process. A total of 1.0 g iron oxide was poured into the three-necked flask, 5 mL distilled water was then added. Then, the solution was stirred until iron oxide nanoparticles well-diversified. After that, 50 mL polyacrylamide was added into the solution drop wise in about 20 min and the mixture was vigorously stirred (800 rpm) for 10 min. The solid and liquid were separated by external magnetic field and the PMMN was obtained then.

In order to find a suitable polyacrylamide concentration at which iron oxide was effectively modified, iron oxide was stirred with different concentration (0–600 mg L^{-1}) of polyacrylamide solution. The Cr(VI) removal percentage was taken as evaluation parameter.

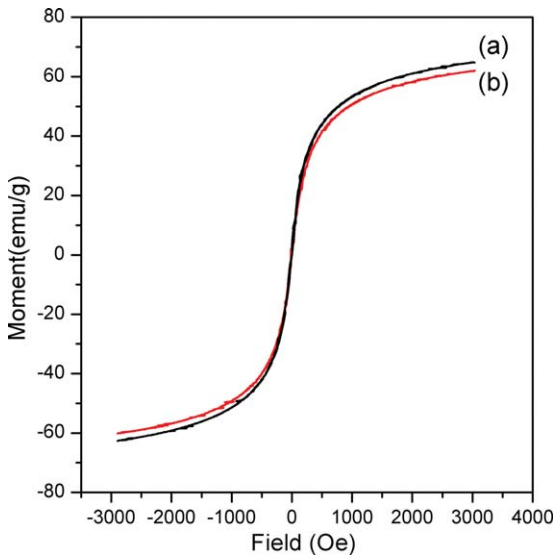

Figure 4. VSM measurement for synthesized iron oxide (a) and PMMN (b). [Color figure can be viewed in the online issue, which is available at wileyonlinelibrary.com.]

Adsorption Studies

Adsorption studies were conducted with a batch method. The experiment was performed by adding the 1.0 g prepared PMMN to 50 mL (100 mg L^{-1}) Cr(VI) solution ($K_2Cr_2O_7$) in 100 mL conical flasks. The conical flasks were set on a shaker. They were shaken for 40 min at 250 rpm in a temperature of 30°C. The pH of the solution was adjusted by 0.1*M* NaOH and 0.1*M* H_2SO_4. The supernatant solution and adsorbent were magnetic separated. Then, the supernatant was analyzed by UV–Vis spectrophotometer (V-1800, Mapada) using 1,5-diphenylcarbazide method.[20]

The effect of pH on adsorption of Cr(VI) studies were performed by adjusting the pH of the solution to 1–8. For adsorption kinetics studies, the prepared PMMN was added into Cr(VI) solution with contact time ranging from 0 to 120 min. The supernatant solution was taken for Cr(VI) concentration measurement at specific time intervals. Isotherm studies were conducted by varying the Cr(VI) initial concentration (50–1000 mg L^{-1}) at 30°C. The effect of coexisting ions on adsorption of Cr(VI) studies were performed by adding different concentrations of salts into the solution under the optimal condition. All the experiments were carried out in triplicate. The percentage removal of Cr(VI) was calculated as follows:

$$R_{Cr(VI)}\% = \left[\frac{C_0 - C_e}{C_0}\right] \times 100 \quad (5)$$

and adsorption capacity values of the adsorbent were calculated using the following equation:

$$q_e = \frac{(C_0 - C_e)V}{w} \quad (6)$$

where q_e is the adsorption amount (mg g^{-1}) when equilibrium is reached, C_0 and C_e are the initial and equilibrium Cr(VI)

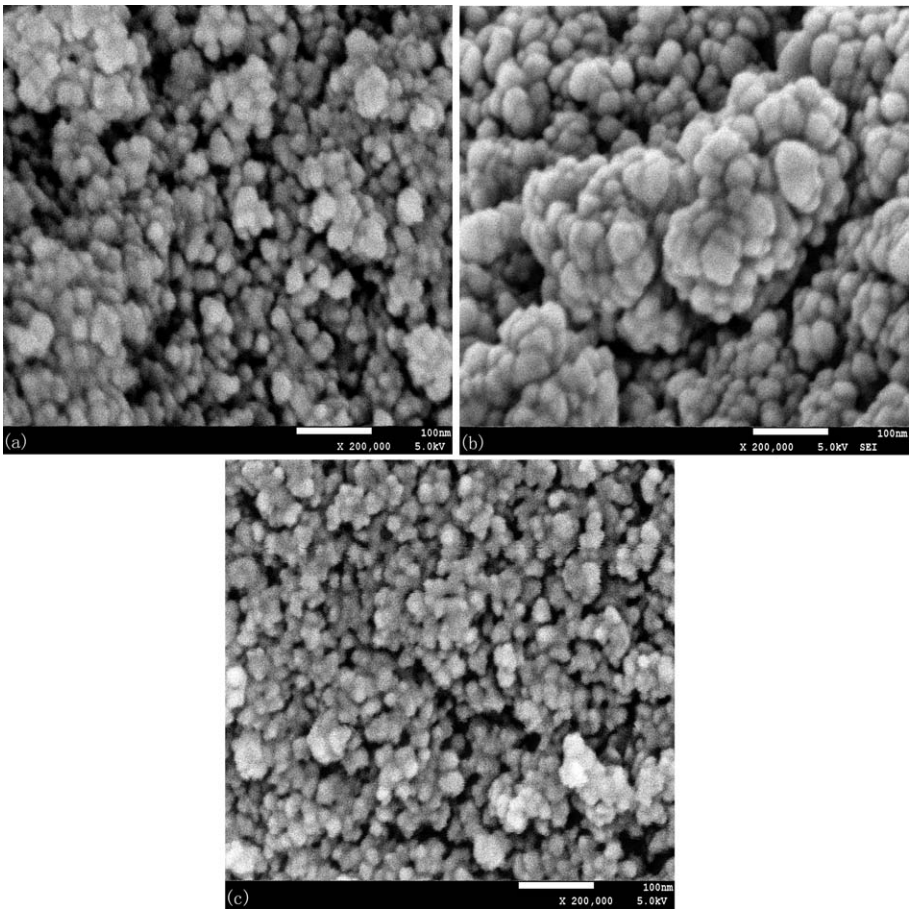

Figure 6. SEM images of the synthesized iron oxide (a), PMMN before (b), and after (c) adsorption.

concentrations (mg L^{-1}), respectively. V is the volume of solution (L) and w is the dose of the adsorbent (g).

Desorption Studies

Desorption studies were carried out by mixing 1 g Cr(VI)-loaded adsorbent and 25 mL 0.1*M* NaOH and shaking for 5 h at 250 rpm. After equilibrium was attained, the sorbent was magnetically separated and washed with distilled water. The regenerated sorbent was reused for adsorption. Loading-regeneration cycle was repeated three times. The percentage removal of Cr(VI) was calculated as eq. (5). And desorption efficiency was calculated according to:

$$\text{desorption effeciency}\% = \frac{C_{ed} V_d}{q_e w} \times 100 \quad (7)$$

where C_{ed} (mg L^{-1}) is the equilibrium concentration after desorption, V_d (L) is the volume of the eluant, q_e is the adsorption amount (mg g^{-1}) when adsorption equilibrium is reached, and w is the dose of the adsorbent (g).

Characterization Methods

All the samples were characterized after drying. Fourier transformed infrared (FTIR) spectra were recorded on a WOF-520 spectrometer using KBr pellets. X-ray diffraction (XRD) (PANalytical X' Pert PRO) was used for the analysis of elemental information and structure at ambient temperature. The instrument was equipped with a copper anode generating Cu Kα radiation ($\lambda = 1.5406$ Å). Magnetic behavior was determined by VSM (HH-10). The thermal gravity analysis/differential thermal gravity (TG/DTG) analyses were conducted under air atmosphere on a TG (NETZSCH STA 449F3) instrument. Morphology and grain size of the samples were examined by SEM (JSM-7500F) at 5.0 kV. Energy dispersive spectroscopy (EDS) coupled to the SEM was used to identify the element composition. X-ray photoelectron spectroscopy (XPS) (AXIS Ultra DLD) was used for the analysis of elemental composition and chemical oxidation state of surface and near-surface species. The XPS measurement was made with an Al Kα X-ray source at a constant retard ratio of 40.

RESULTS AND DISCUSSION

Effect of PAM Concentration on Cr(VI) Removal

As Lee and Sonasundaran[21] reported, the electronegative C═O group of polyacrylamide could connected with the hydroxyl on the surface of iron oxide by H bonding. In this work, the synthesized iron oxide was modified by polyacrylamide with different polyacrylamide concentration (0–600 mg L^{-1}). It was clear from Figure 1 that the Cr(VI) removal percentage reached the maximum when the polyacrylamide concentration increased to

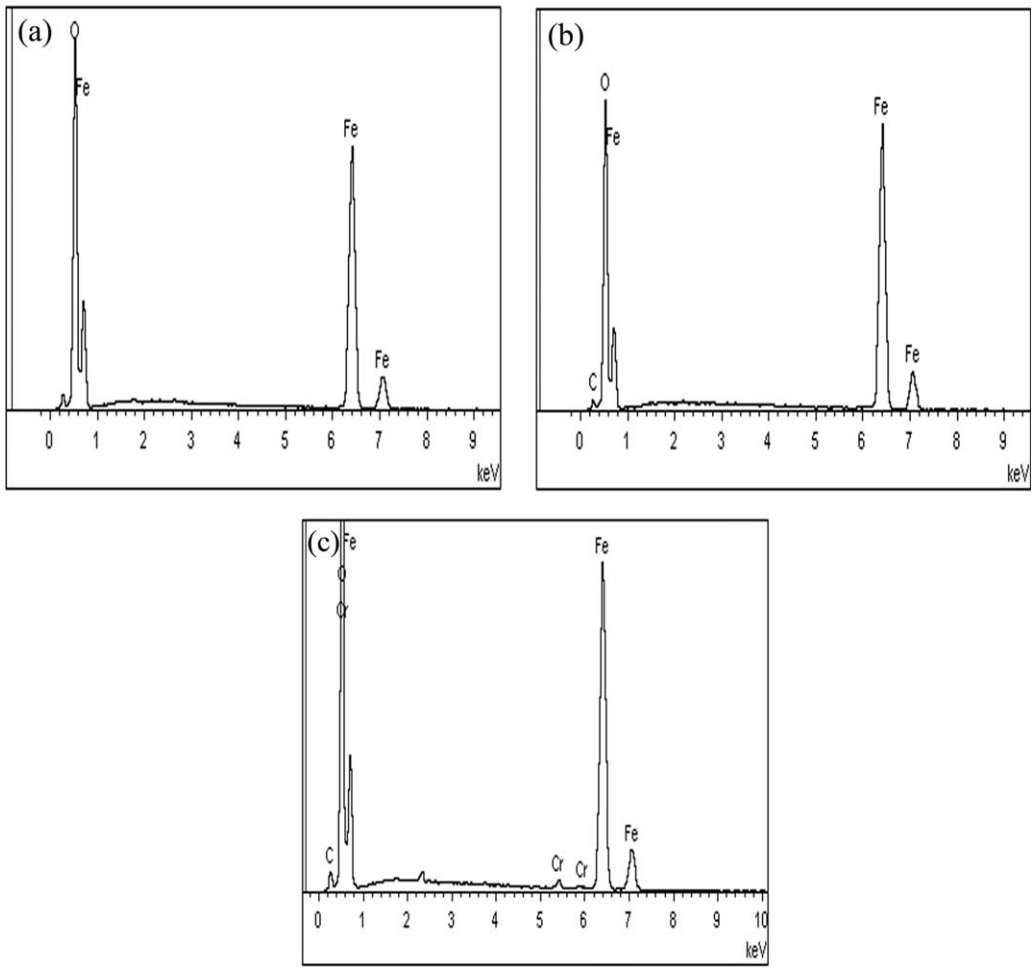

Figure 7. EDS spectrum of synthesized iron oxide (a), PMMN before (b), and after (c) adsorption.

400 mg L^{-1}. There was no evident change in removal percentage as the polyacrylamide concentration continued to increase. This may be because that along with the increase of polyacrylamide concentration, the amount of polyacrylamide covered on the iron oxide increased. As a result, the removal percentage increased. When the concentration increased to 400 mg L^{-1}, the amount of polyacrylamide adsorbed on iron oxide reached the maximum. So the removal percentage reached the maximum. However, increasing concentration could not make the amount of polyacrylamide adsorbed on the iron oxide increase. Therefore, continuing to increase concentration had no effect on removal percentage.

In addition, we measured the completely settling time of both synthesized iron oxide and PMMN under the same condition. From Table I, settling time were 4 min and 16 s for synthesized iron oxide and PMMN, respectively. These data illustrated our advantage well.

Characterization

The FTIR spectrum of the synthetic iron oxide and PMMN was showed in Figure 2. The strong and sharp peak at 573 cm^{-1} in Figure 2(a) was the characteristic absorption peak of iron oxide. Obviously, the FTIR spectrum of the PMMN, Figure 2(b), had difference with the iron oxide. The wide adsorption band at about 3422 cm^{-1} was on account of N—H stretching vibration of amide. And 1641 cm^{-1} absorption peak can be assigned to the overlapping of C═O stretching vibration and N—H bending vibration in amide. The wide and strong adsorption band at 583 cm^{-1} was iron oxide characteristic absorption peak. This revealed that the iron oxide had been successfully modified with polyacrylamide.

Figure 3 shows the results of XRD analysis for the synthesized iron oxide (a) and PMMN (b). The XRD patterns of synthesized iron oxide showed eight characteristic peaks at 2θ of 18.2°, 30.2°, 35.5°, 43.3°, 53.7°, 57.2°, 62.8°, and 74.4° corresponding to their indices (111), (220), (311), (400), (422), (511), (440), and (533). They matched well with standard Fe_3O_4 without other crystalline phases appearing. The XRD image of PMMN was similar to synthesized iron oxide. This suggested that the modification of the synthesized iron oxide did not make significant changes of crystal structure on iron oxide.

Figure 4 presents the magnetization loop for the synthesized iron oxide (a) and PMMN (b), where no remanence and coercivity were detected. From Figure 4, we found that the

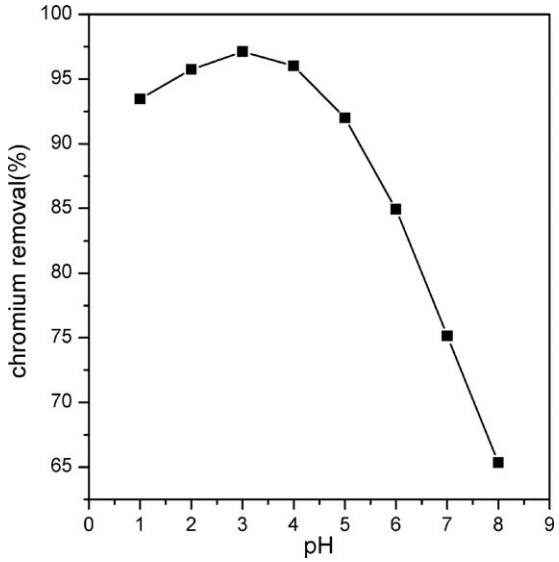

Figure 8. Effect of pH on the removal of Cr(VI). Polyacrylamide concentration, 400 mg L^{-1}; Cr(VI) concentration, 100 mg L^{-1}; contact time, 40 min at 30°C.

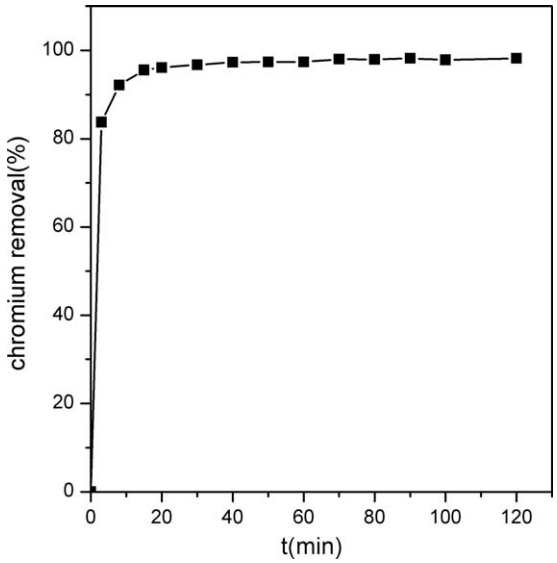

Figure 9. Effect of contact time on the removal of Cr(VI). Polyacrylamide concentration, 400 mg L^{-1}; Cr(VI) concentration, 100 mg L^{-1}; pH 3 at 30°C.

saturation moment of per gram PMMN (62.02 emu g^{-1} at 3043Oe) was smaller than synthesized iron oxide (64.89 emu g^{-1} at 3009Oe). This was very easy to explain. Polyacrylamide was not magnetic. The amount of iron oxide in PMMN was less than 1 g. Its saturation moment was naturally less than 1 g of iron oxide. The large saturation magnetization and superparamagnetic property of the PMMN made it susceptible to magnetic field and easily separate with liquid phase.

The TG/DTG analyses of the synthesized iron oxide (a) and PMMN (b) were shown in Figure 5. It can be seen that the mass loss completing at 180°C were 3.72% and 4.90% for synthesized iron oxide and PMMN, respectively. They were attributed to free water and bound water. For synthesized iron oxide, the mass losses from 390°C to 480°C and from 480°C to 717°C were ascribed to surface dehydroxylation. The mass losses were 0.41% and 1.17% and the ratio was close to 1 : 2. So they were thought to be the loss of hydroxyl group bonded to Fe^{2+} and Fe^{3+}, respectively. With regard to PMMN, the large loss between 180°C and 390°C was assigned to the degradation of polyacrylamide and the loss of hydroxyl bonded to polyacrylamide. This was because the bonding between iron oxide and hydroxyl bonded to polyacrylamide became weaker after modification. The mass loss (480–636°C) was attributed to the loss of hydroxyl of iron oxide. From Figure 5, we can figure out the polyacrylamide content of PMMN was about 1.57%.

The SEM spectra of synthesized iron oxide (a), PMMN before (b) and after (c) adsorption Cr(VI) were given in Figure 6. From Figure 6, we can see that both synthesized iron oxide and the PMMN were nanoscale. As shown in Figure 6(a), the diameter of the synthesized iron oxide was about 20 nm and the shape was approximately spherical. Making a comparison of Figure 6(a,b), we found that the particles were more aggregated in Figure 6(b). This may be because multiple iron oxide was wrapped in the long chain of polyacrylamide. In other words, polyacrylamide pull together the dispersed iron oxide. In Figure 6(c), the particles were tighter than Figure 6(a), but less aggregated than Figure 6(b). This was because a large number of $HCrO_4^-$ (e.g.) ions entered into the aggregated group and adsorbed by it. The aggregated group was divided by these ions via electrostatic repulsion. Figure 7 is the EDS spectra of

Table II. Comparison of Equilibrium Time

Material	Equilibrium time	Reference
PMMN	40 min	This work
Mixed maghemite-magnetite	120 min	16
Activated carbons	150 min	1
Polyethylenimine-modified fungal biomass	180 min	15
Polypyrrole/graphene oxide composite	180 min	10
Polyacrylamide-grafted sawdust	240 min	14
Amine-modified polyacrylamide-grafted coconut coir pith	240 min	13
Lignocellulosic substrate	24 h	8

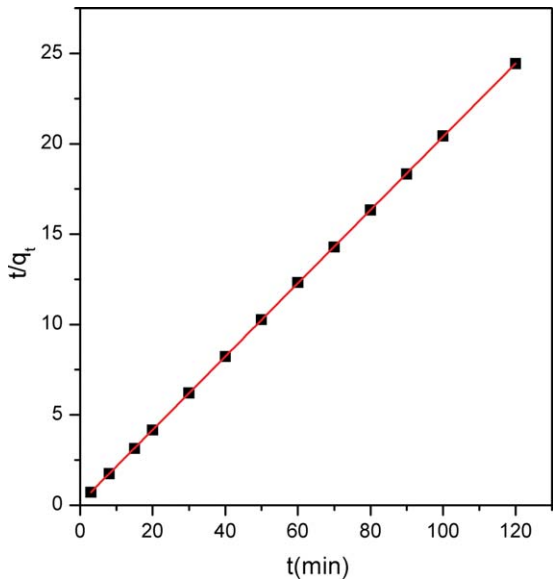

Figure 10. Pseudo-second-order kinetic for the removal of Cr(VI) on PMMN. Polyacrylamide concentration, 400 mg L^{-1}; Cr(VI) concentration, 100 mg L^{-1}; pH 3 at 30°C. [Color figure can be viewed in the online issue, which is available at wileyonlinelibrary.com.]

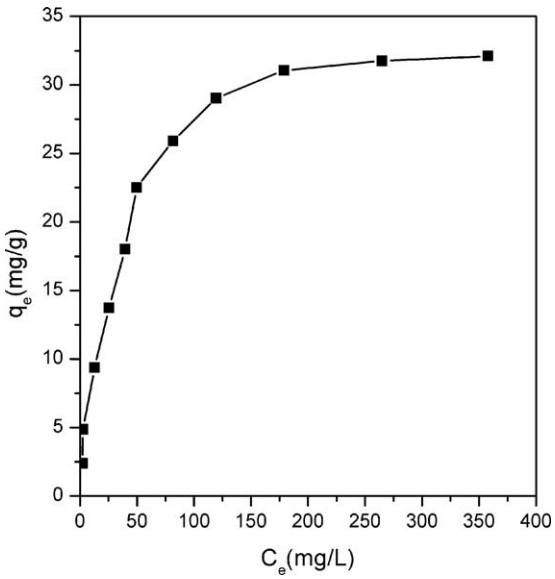

Figure 11. Adsorption isotherm of Cr(VI) adsorption. Polyacrylamide concentration, 400 mg L^{-1}; contact time, 40 min; pH 3 at 30°C.

synthesized iron oxide (a), PMMN before (b), and after (c) adsorption Cr(VI). In Figure 7(a), only O and Fe elements were detected indicating the purity of iron oxide. Due to the limitation of EDS analysis of N element, there was no N in Figure 7(b). But the C element was an indication of successful modification of iron oxide with polyacrylamide. The appearance of Cr element in Figure 7(c) revealed the adsorption of Cr(VI) on PMMN.

Effect of pH on Cr(VI) Removal by PMMN

As is known, pH is an important factor affecting the Cr(VI) adsorption in aqueous phase. In order to study the effect of pH on its adsorption capacity by PMMN, adsorption experiments were conducted by varying the pH from 1 to 8, and the result was shown in Figure 8. It was clear from Figure 8 that the Cr(VI) removal percentage was obviously better under acidic conditions. From 1.0 to 3.0, the Cr(VI) removal percentage increased slightly with the increase of pH and reached the maximum at pH 3.0. Then, Cr(VI) removal percentage decreased significantly as pH increased from 3.0 to 8.0.

Reasons for this phenomenon may be various. Cr(VI) existed in water as H_2CrO_4, $HCrO_4^-$, CrO_4^{2-}, $Cr_2O_7^{2-}$, etc.[15], almost of them were anion. The pH_{zpc} of PMMN was 4.5. Under the pH_{zpc}, the PMMN surface was positively charged forming numbers of $-NH_3^+$, Fe^{2+}, and $FeOH^+$ groups. So the anion adsorption is favored as below:

$$PMMN-NH_3^+ + HCrO_4^- \rightarrow PMMN-NH_3^+ \cdots HCrO_4^- \quad (8)$$

$$PMMN-FeOH^+ + HCrO_4^- \rightarrow PMMN-FeOH^+ \cdots HCrO_4^- \quad (9)$$

And the removal percentage decreased rapidly when the $pH > pH_{zpc}$. On the other hand, Chowdhury et al.[16] reported that the adsorption free energy of $HCrO_4^-$ is lower than CrO_4^{2-}. Thus, $HCrO_4^-$ is more favorably adsorbed than CrO_4^{2-} at the same concentration. At lower pH, parts of CrO_4^{2-} changed into $HCrO_4^-$. This made more Cr(VI) adsorbed. So the decrease of pH leads to the increase of Cr(VI) removal percentage. However, when the $pH < 3$, parts of the excess H^+ combined with $HCrO_4^-$, CrO_4^{2-}, $Cr_2O_7^{2-}$, developing H_2CrO_4 and $H_2Cr_2O_7$. They were uncharged and could not be adsorbed. So the Cr(VI) removal percentage decreased.

Adsorption Kinetics of Cr(VI) Removal by PMMN

Because adsorption equilibrium time was an economic factor for wastewater treatment plant, the effect of contact time on the Cr(VI) uptake was studied. Result was presented in Figure 9. It can be found that the rate of Cr(VI) uptake was very quick at the beginning, and 97% Cr(VI) was removed within about 30 min. Then, equilibrium was reached after 40 min. We made a rough comparison of equilibrium time. Result was presented in Table II. The rapid Cr(VI) uptake may caused by external surface adsorption, which was different from interior adsorption by porous adsorbent. Once the adsorbate reached the PMMN surface and contacted with active site, the adsorption took place. But for porous adsorbent whose active site was inside, the adsorbate had to get into the porous adsorbent then could be adsorbed.

In order to investigate the adsorption kinetics, pseudo-second-order kinetic model was used to evaluate the experimental data. The equation was expressed as follow:

$$\frac{t}{q_t} = \frac{1}{k_2 q_e^2} + \frac{t}{q_e} \quad (10)$$

where q_e and q_t were the amount of Cr(VI) adsorbed (mg g^{-1}) at equilibrium and at time t, respectively. k_2 was the rate constant of adsorption (g mg^{-1} min^{-1}). Result was given in Figure 10. The value of k_2 and q_e were 0.3716 and 4.930, respectively. The calculative q_e (4.930) was very close to the experimental q_e

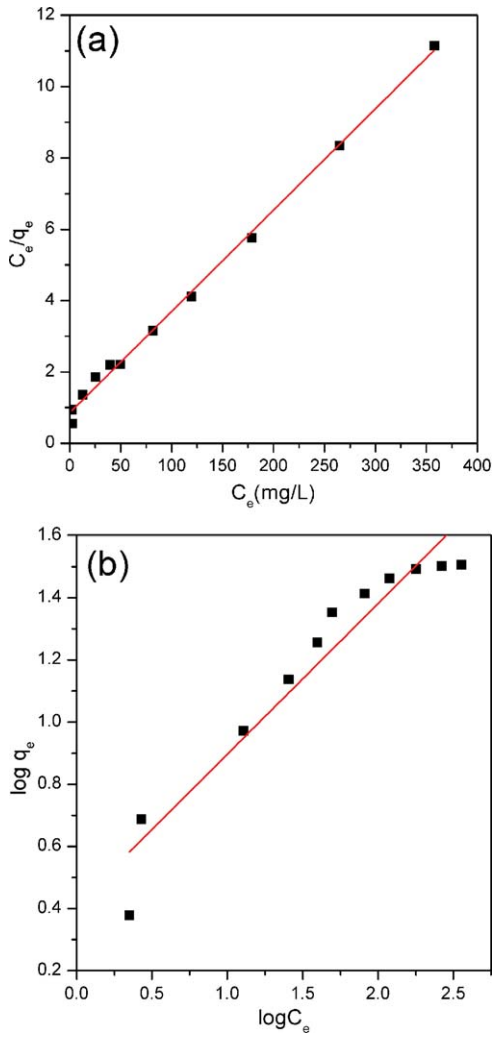

Figure 12. Langmuir (a) and Freundlish (b) isotherm of Cr(VI) adsorption on the PMMN. Polyacrylamide concentration, 400 mg L^{-1}; contact time, 40 min; pH 3 at 30°C. [Color figure can be viewed in the online issue, which is available at wileyonlinelibrary.com.]

(4.8652). Moreover, the correlation coefficient for the linear fitting the data with this model was 0.9999. It revealed that this model could well describe the adsorption kinetics performance. With this model, it was demonstrated that the adsorption occurred by a monolayer regime on the adsorption surface.[22]

Adsorption Isotherm of Cr(VI) Removal by PMMN

The adsorption behavior and adsorption capacity of Cr(VI) on the adsorbent was studied. Experiments for adsorption isotherm were carried out by varying the Cr(VI) initial concentration (50–1000 mg L^{-1}) at 30°C, pH 3. Result showed that the Cr(VI) removal efficiency dropped from 98.30% to 64.20% when Cr(VI)

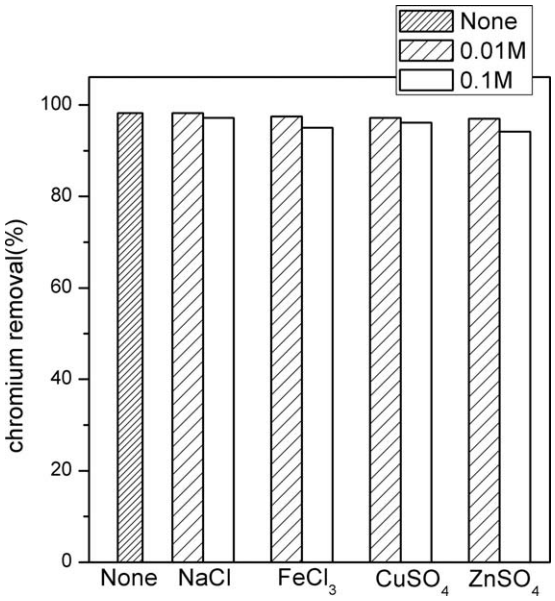

Figure 13. Effect of coexisting salts on Cr(VI) removal by PMMN. Polyacrylamide concentration, 400 mg L^{-1}; Cr(VI) concentration, 100 mg L^{-1}; contact time, 40 min; pH 3 at 30°C.

initial concentration was increased from 50 mg L^{-1} to 1000 mg L^{-1}. Thus, Cr(VI) removal was highly concentration-dependent. The relationship of C_e and q_e was depicted by Figure 11. As can be seen from Figure 11, q_e increased rapidly at the beginning. Then, the increase tended to slow and finally reached to the maximum (i.e., the maximum adsorption capacity).

Langmuir and Freundlich isotherm were used to fit the experimental data and expressed as the following eqs. (11) and (13), respectively.

$$\frac{C_e}{q_e} = \frac{b}{q_{\max}} + \frac{C_e}{q_{\max}} \tag{11}$$

where the q_e was the amount of Cr(VI) adsorbed by per unit weight of sorbent (mg g^{-1}) at equilibrium, C_e was the equilibrium Cr(VI) concentrations (mg L^{-1}) left in the solution. $q_{\max}$ was the maximum amount of Cr(VI) adsorbed by per unit weight of sorbent (mg g^{-1}) and the constant b related to the binding energy. $q_{\max}$ and b can be determined from the slope and the intercept of the linear plot between C_e/q_e and C_e.

The adsorption intensity (R_L) can be expressed as:

$$R_L = \frac{1}{1+bC_0} \tag{12}$$

where C_0 (mg L^{-1}) was the initial concentration. The average value of R_L indicated the types of Langmuir isotherm of irreversible ($R_L = 0$), favorable ($0 < R_L < 1$), linear ($R_L = 1$), or unfavorable ($R_L > 1$).[23]

Table III. Langmuir and Freundlish Isotherm Constants for the Adsorption of Cr(VI)

Langmuir isotherm					Freundlish isotherm			
$q_{\max}$ (mg g^{-1})	b (L mg^{-1})	R^2	R_L	Δq (%)	K_f (mg g^{-1})	n	R^2	Δq (%)
35.186	29.982	0.996	0-1	14.316	2.582	2.064	0.919	25.242

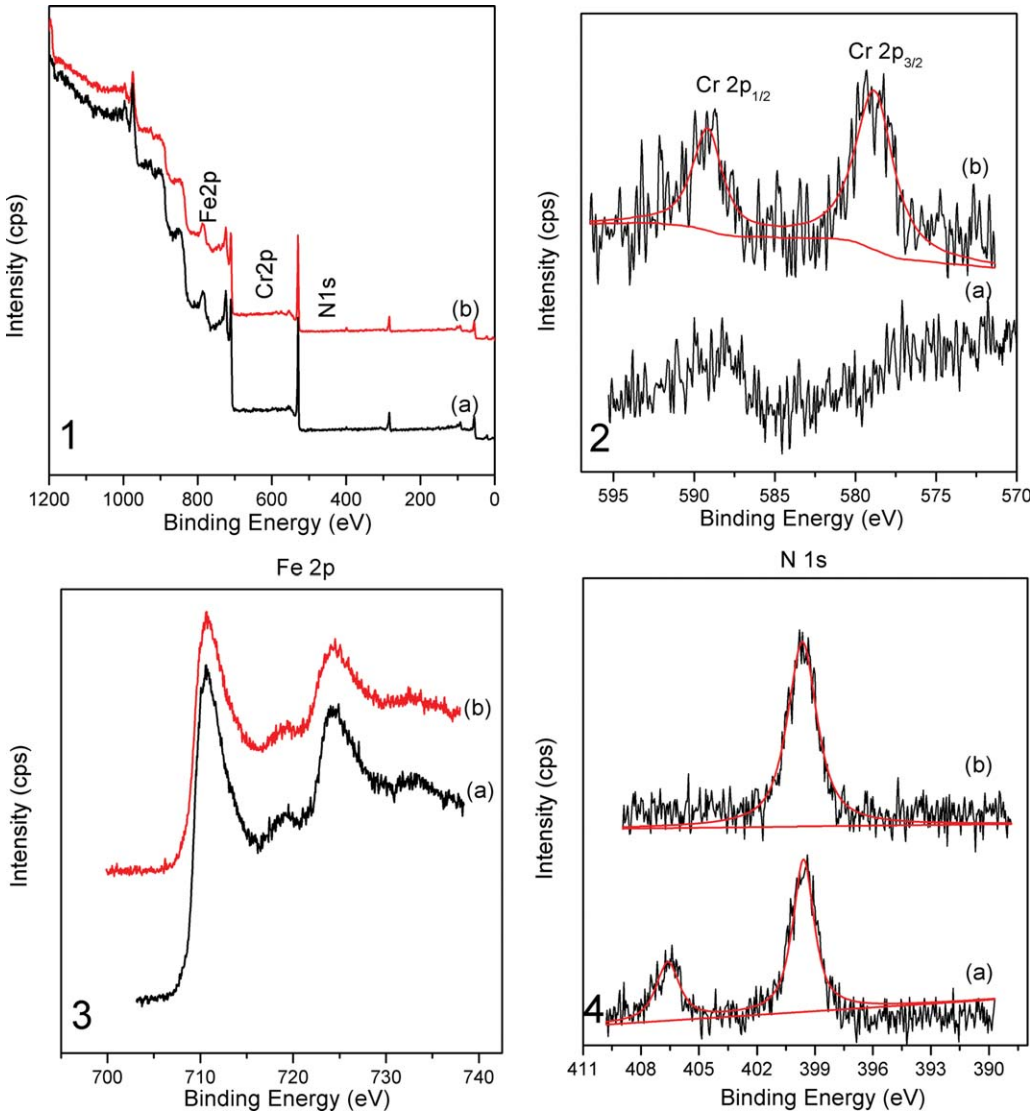

Figure 14. The XPS spectra of samples. (1) The XPS spectra of PMMN before (a) and after (b) adsorption. (2) The XPS spectra of Cr in PMMN before (a) and after (b) adsorption. (3) The XPS spectra of Fe in PMMN before (a) and after (b) adsorption. (4) The XPS spectra of N in PMMN before (a) and after (b) adsorption. [Color figure can be viewed in the online issue, which is available at wileyonlinelibrary.com.]

Freundlish isotherm was represented as:

$$\log q_e = \log K_f + \frac{1}{n}\log C_e \tag{13}$$

where q_e was the amount of Cr(VI) adsorbed by per unit weight of sorbent (mg g^{-1}) at equilibrium, C_e was the equilibrium concentration of Cr(VI) (mg g^{-1}). K_f (mg g^{-1}) and n were Freundlish constants related to the capacity of adsorption and favorability of adsorption, respectively. A normalized standard deviation, Δq (%), was used to compare the validity of the isotherm models and was calculated by:

$$\Delta q(\%) = 100 \times \sqrt{\frac{\sum \left[\left(q_e^{\exp} - q_e^{\mathrm{cal}}\right)/q_e^{\exp}\right]^2}{N}} \tag{14}$$

where $q_e^{\exp}$ and q_e^{cal} were the experimental and calculated q_e value, N was the number of experimental data. Langmuir and Freundlish isotherm of Cr(VI) adsorption by the PMMN were shown in Figure 12. The fitted results, the value of R_L, Δq were given in Table III.

The value of R_L (0–1) and the value of n (0–1) indicated that Cr(VI) was favorably adsorbed. These two isotherms fitted well with the experimental data according to the correlation coefficient R^2. However, Langmuir isotherm fitted better than Freundlish isotherm when taking Δq into consideration. And this was obvious from Figure 12. This revealed that the Cr(VI) uptake followed a monolayer adsorption on a homogenous surface without any interaction between adsorbed ions.[23] From Table III, the maximum adsorption of Cr(VI) ion by PMMN, $q_{\max}$ (35.186 mg g^{-1}), is higher than those of activated carbon[24] (3.46 mg g^{-1}), sawdust[25] (3.6 mg g^{-1}), maghemite[23] (17.43 mg g^{-1}), and modified $MnFe_2O_4$[26] (31.55 mg g^{-1}).

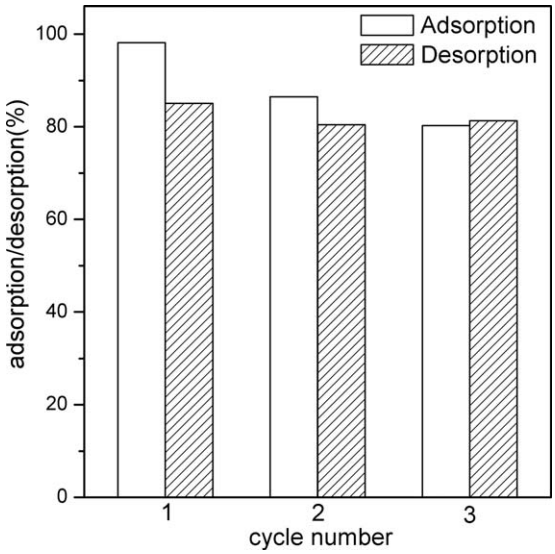

Figure 15. Regeneration study of PMMN.

Effect of Coexisting Salts on Cr(VI) Removal by PMMN

Wastewater containing Cr(VI) always had many other metal ions (e.g., electroplating wastewater). The effect of them on Cr(VI) removal should be taken into consideration. In this article, 0.01*M* and 0.1*M* NaCl, $FeCl_3$, $CuSO_4$, and $ZnSO_4$ were added into solution, respectively. Results were shown in Figure 13. From Figure 13, we found that there was almost no effect of these salts on Cr(VI) removal at the low concentration. The effect was more apparent when the concentration of salt was 10 times as big as the low concentration. This may be the result of competition between ions. The chances of Cr(VI) contacting with adsorbent reduced when salt concentration increased. This finally leads to the decrease of Cr(VI) removal. However, even at concentration of 0.1*M*, the decrease was not big.

Adsorption Mechanism of Cr(VI) Removal by PMMN

To investigate the adsorption mechanism of Cr(VI), the XPS spectra of the PMMN before and after adsorption of Cr(VI) were presented in Figure 14. After comparing Figure 14(3a,b), we found that there was no evident shift of the Fe(2p) peak. This indicated that no change in Fe on structure and valence. On the contrary, the N(1s) peak changed in Figure 14(4). This revealed that the environment of N element changed. Furthermore, the Cr(2p3/2) peak centered at 578.8 eV and Cr(2p1/2) peak centered at 589.2 eV were contributed to the Cr(VI) in Figure 14(2b). This suggested that there was no change in valence of Cr(VI). In other words, there was no chemical redox reaction undergoing the adsorption after analyzing XPS spectra.

On the other hand, the total chromium was determined later. It was very close to the amount of Cr(VI) and the difference was below 2%. This suggested that a small amount of Cr(VI) was reduced to Cr(III) during the process. Therefore, the mechanism of Cr(VI) uptake onto PMMN was proposed to be adsorption-coupled reduction.

Adsorbent Regeneration

Considering the economy, we studied the regeneration of sorbent. The adsorption and desorption data were presented in Figure 15. It showed a gradual decrease in Cr(VI) adsorption with increase in cycle number. Lee and Sonasundaran[21] reported that the adsorption of polyacrylamide on iron oxide decreased with an increase in pH. So we suspected that polyacrylamide dropped from iron oxide during the regeneration. And this made the Cr(VI) removal efficiency reduce to 86.51% after the first desorption. Until the third cycle, particles were smaller and the sedimentation rate was slower. There was almost no polyacrylamide on the iron oxide. These phenomena indicated that the regeneration of PMMN was not that feasible. However, the iron oxide after desorption could be reused to prepare PMMN.

CONCLUSION

In this study, iron oxide was successfully modified by polyacrylamide and the efficiency of the PMMN removing Cr(VI) was investigated. The results showed that the Cr(VI) uptake by PMMN was highly pH, contact time, and initial Cr(VI) concentration dependent. The process followed pseudo-second-order kinetics model and the equilibrium time was 40 min. Langmuir and Freundlich isotherm were used to fit the experimental data and Langmuir isotherm fitted better than Freundlich. The maximum adsorption amount of Cr(VI) by PMMN was 35.186 mg/g. The effect of coexisting salts on Cr(VI) removal was not apparent even the concentration of salt was 10 times as big as the low concentration, 0.01*M*. After analysis XPS spectra of the PMMN before and after adsorption of Cr(VI), it was proposed that the mechanism of Cr(VI) uptake onto PMMN was adsorption-coupled reduction. Above all, PMMN is a promising adsorbent to remove Cr(VI) with the characteristics of fast, economic, and efficient.

ACKNOWLEDGMENTS

This work was supported by Open Fund (PLN1134) of State Key Laboratory of Oil Gas Reservoir Geology and Exploitation (Southwest Petroleum University) of China and Sichuan Provincial Scientific and Technological Transformational Achievements Project (S688) and SWPU Pollution Control of Oil & Gas Fields Science & Technology Innovation Youth Team (Number: 2013XJZT003).

REFERENCES

1. Khezami, L.; Capart, R. *J. Hazard. Mater.* **2005**, *B123*, 223.
2. Béni, Á.; Karosi, R.; Posta, J. *Microchem. J.* **2007**, *85*, 103.
3. Nakano, Y.; Takeshita, K.; Tsutsumi, T. *Water Res.* **2001**, *35*, 496.
4. Ramakrishnaiah, C. R.; Prathima, B. *Int. J. Eng. Res. Appl.* **2012**, *2*, 599.
5. Beukes, J. P.; Pienaar, J. J.; Lachmann, G.; Giesekke, E. W. *Water SA* **1999**, *25*, 363.
6. Barrera-Díaz, C.; Palomar-Pardavé, M.; Romero-Romo, M.; Martínez, S. *J. Appl. Electrochem.* **2003**, *33*, 61.
7. Eisazadeh, H. *J. Appl. Polym. Sci.* **2007**, *104*, 1964.
8. Dupont, L.; Guillon, E. *Environ. Sci. Technol.* **2003**, *37*, 4235.

9. Chauhan, D.; Sankararamakrishnan, N. *J. Hazard. Mater.* **2011**, *185*, 55.
10. Li, S.; Lu, X. F.; Xue, Y. P.; Lei, J. Y.; Zheng, T.; Wang, C. *PLoS One* **2012**, *7*, 1.
11. Zhao, Y. L.; Gao, Q.; Tang, T.; Xu, Y.; Wu, D. *Mater. Lett.* **2011**, *65*, 1045.
12. Li, H. D.; Li, Z.; Liu, T.; Xiao, X.; Peng, Z. H.; Deng, L. *Bioresour. Technol.* **2008**, *99*, 6271.
13. Unnithan, M. R.; Vinod, V. P.; Anirudhan, T. S. *Ind. Eng. Chem. Res.* **2004**, *43*, 2247.
14. Raji, C.; Anirudhan, T. S. *Water Res.* **1998**, *32*, 3772.
15. Deng, S. B.; Ting, Y. P. *Environ. Sci. Technol.* **2005**, *39*, 8490.
16. Chowdhury, S. R.; Yanful, E. K.; Pratt, A. R. *J. Hazard. Mater.* **2012**, *235-236*, 246.
17. Anirudhan, T. S.; Rijith, S.; Suchithra, P. S. *J. Appl. Polym. Sci.* **2009**, *115*, 2069.
18. Zhao, Y.-G.; Shen, H.-Y.; Pan, S.-D.; Hu, M.-Q. *J. Hazard. Mater.* **2010**, *182*, 295.
19. Li, Y.-S.; Church, J. S.; Andrea L. *J. Magn. Magn. Mater.* **2012**, *324*, 1543.
20. Geng, B.; Jin, Z. H.; Li, T. L.; Qi, X. H. *Chemosphere* **2009**, *75*, 825.
21. Lee, L. T.; Sonasundaran, P. *Langmuir* **1989**, *5*, 854.
22. Phuengprasop, T.; Sittiwong, J.; Unob, F. *J. Hazard. Mater.* **2011**, *186*, 502.
23. Hu, J.; Chen, G. H.; Irene, M. C. L.; Asce, M. *J. Environ. Eng.* **2006**, *132*, 709.
24. Selvi, K.; Pattabhi, S.; Kadirbelu, K. *Bioresour. Technol.* **2001**, *80*, 87.
25. Baral, S. S.; Das, S. N.; Rath, P. *Biochem. Eng. J.* **2006**, *31*, 216.
26. Hu, J.; Irene, M. C. L.; Chen, G. H. *Langmuir* **2005**, *21*, 11173.